Empirical Constraints on Progressive Shock Metamorphism of Magnetite from the Siljan Impact Structure, Sweden

Sanna Holm-Alwmark[1,2,3], Timmons M. Erickson[4,5], and Aaron J. Cavosie[5]

[1]Niels Bohr Institute, University of Copenhagen, Blegdamsvej 17, 2100 Copenhagen, Denmark

[2]Department of Geology, Lund University, Sölvegatan 12, 22362 Lund, Sweden

[3]Natural History Museum Denmark, University of Copenhagen, Copenhagen, Denmark

[4]Jacobs – JETS, NASA Johnson Space Center, Astromaterials Research and Exploration Science Division, Mailcode XI3, 2101 NASA Parkway, Houston, TX, 77058 USA,

[5]Space Science and Technology Centre, The Institute for Geoscience Research (TIGeR), School of Earth and Planetary Sciences, Curtin University, Perth, GPO Box U1987, WA 6845, Australia.

ABSTRACT

Little is known about the microstructural behavior of magnetite during hypervelocity impact events, even though it is a widespread accessory mineral and important magnetic carrier in terrestrial and extraterrestrial rocks. We report systematic electron backscatter diffraction crystallographic analysis of shock features in magnetite, from a transect across the 52-km-diameter ~380 Ma Siljan impact structure in Sweden. Magnetite grains in granitoid samples contain brittle fracturing, crystal-plasticity, and lamellar twins. Deformation twins along {111} with shear direction of <112> are consistent with spinel-law twins. Inferred bulk shock pressures for investigated samples, as constrained by planar deformation features (PDFs) in quartz and shock twins in zircon, range from 0–20 GPa; onset of shock-induced twinning in magnetite is observed at >5 GPa. These results highlight the utility of magnetite to record shock deformation in rocks that experience shock pressures >5 GPa, which may be useful in quartz-poor samples. Despite significant hydrothermal alteration, and variable transformation of host magnetite to hematite, shock effects are preserved, demonstrating that magnetite is a reliable mineral for preserving shock deformation over geologic time.

INTRODUCTION

Magnetite, with an inverse spinel structure and nominal chemical formula of $Fe_2^{3+}Fe^{2+}O_4^{2-}$, is a common accessory mineral in igneous, sedimentary, and metamorphic rocks (e.g., Deer et al., 1992). It forms under a wide range of conditions and is one of the most important magnetic carriers in both terrestrial and extraterrestrial rocks (e.g., Dunlop and Özdemir, 1997; Louzada et al., 2011). Magnetite, alongside other ferromagnetic minerals, defines magnetic anomalies associated with impact craters on Earth and other bodies that are essential to the discovery and mapping of such features (e.g., Pilkington and Grieve, 1992). Deformation can modify the magnetic signature of rocks on Earth, e.g., in tectonic pseudotachylites (e.g., Ferré et al., 2005), and shock deformation may permanently alter intrinsic magnetic properties of rocks (e.g., Gilder et al., 2004; Kletetschka et al., 2004; Gattacceca et al., 2007; Reznik et al., 2016). Yet, detailed microstructural characterization of shock deformation in magnetite is limited to one experimental study (Reznik et al., 2016).

Here we use scanning electron microscopy (SEM)-based electron backscatter diffraction (EBSD) analysis to conduct a systematic assessment of shock microstructures in magnetite from the Siljan impact structure. We document microstructural shock effects in magnetite from granitoid rocks from the central uplift of a large (>50 km diameter) impact structure. As the samples have well-constrained shock pressure estimates based on systematic studies of quartz (Holm et al., 2011), we are able to correlate progressive deformation of magnetite with increasing shock pressure.

GEOLOGICAL SETTING, SAMPLES AND METHODS

Siljan is a ~52 km-diameter impact structure located in Sweden (Fig. 1) which formed 380.9 ± 4.6 Myr ago (Reimold et al., 2005; Jourdan, 2012; Holm-Alwmark, 2021, and references therein). Target rocks are crystalline basement rocks that were overlain by a ~3 km thick sequence of sedimentary rocks (Holm-Alwmark et al., 2017). Siljan consists of a 32-km wide central plateau surrounded by an annular depression partly filled by lakes. The area has not undergone any large-scale post-impact tectonic deformation. Four granitoid samples from outcrop in the central plateau of Siljan were investigated (Fig. 1; Table 1; DR Item 1). Samples 69, 21, and 58 were previously assigned to a shock pressure range of 5 to 20 GPa based on PDFs in quartz (Holm et al., 2011; Holm-Alwmark et al., 2018). Sample 5 is from outside the annular depression, beyond the domain of shock metamorphism.

Mineral phase information, crystallographic orientation, and microstructural data by EBSD were collected with a Tescan Mira3 field emission SEM equipped with an Oxford Instruments EBSD detector. Details of operating conditions are specified in DR Items 2, 7.

RESULTS

Up to 10-20 magnetite grains were surveyed in each sample by backscattered electron (BSE) imaging, and orientation mapping using EBSD was conducted on 2-6 representative magnetite grains per sample. Investigated grains are subhedral to euhedral and 90 to 800 µm in size. Grains are often intergrown with biotite and/or amphibole, accessory apatite and zircon. In samples 21, 58, and 5, magnetite is partly altered to hematite, consistent with observed alteration of biotite and amphibole to chlorite (DR Item 1). Orientation analysis of magnetite-hematite intergrowths shows that the transformation is controlled crystallographically, with $\{111\}_{mag}$ aligned with basal $\{0001\}_{hem}$, and $\langle 110\rangle_{mag}$ aligned with $\langle 10\bar{1}0\rangle_{hem}$ (DR Item 4, 5). The transformation results in four hematite orientation variants systematically aligned with one another, which are readily discernable in pole figures, and consistent with a topotactic martitization transformation (e.g., Barbosa & Lagoeiro, 2010).

Deformation microstructures in magnetite

Non-planar and planar brittle fractures occur in all investigated magnetite grains from shocked and unshocked samples (Figs. 2, 3). Fractures are generally not associated with detectable lattice misorientation, although exceptions include areas with a high density of sets of straight, parallel, closely spaced fractures, which occur in shocked samples. Orientation mapping shows the straight fractures coincide with twin boundaries. Twin lamellae are the most conspicuous microstructure observed, and are only present in the three shocked samples (Table 1; Fig. 2). Twins are polysynthetic, occurring as up to four sets of straight lamellae. Twins generally cross each other without apparent offset, except in some instances where planar fractures along twin planes appear to offset other twins (Fig. 2C). Twins have apparent widths up to 5 µm, crosscut the full length of the host crystal, and some show tapered terminations. The apparent thickness of twins varies between twin sets in the same grain, in the same twin orientation, and between grains, depending on angle of intersection with the polished section. Individual twins can be separated by as little as 2-3 µm.

Twin lamellae and host crystals share a systematic orientation relationship defined by a disorientation (i.e., minimum misorientation) of 60° about <111>. This orientation relationship results in coincidence of several <112> crystallographic directions between host and twin that lie normal to the 180° misorientation axis (Fig. 2f). The 180° misorientation axis aligns with the pole to {111}, consistent with spinel-law twinning, with a {111} compositional/invariant plane (K1) and a <112> shear direction (η1).

Magnetite crystals exhibit intragrain cumulative misorientation, up to 18° as evidenced by dispersion in pole figures (e.g., Fig. 2e). Internal misorientation is frequently most concentrated near grain boundaries or between twin lamellae. Crystal plasticity has also resulted in formation of deformation bands with indistinct boundaries in some crystals (Fig. 3). Well-defined deformation bands have systematic crystallographic disorientation about <111> (Fig. 2e, DR item 6a).

Microstructures in zircon

In sample 69, some magnetite grains are intergrown with zircon. Two zircon grains (Fig. 2 and DR Item 6E) exhibit {112} mechanical twin lamellae, disoriented 65° about <110>. This twin type has only been reported in shocked zircon (e.g., Erickson et al., 2013).

DISCUSSION

Shock-induced microstructures in magnetite

Several types of microstructures were observed in magnetite from the Siljan impact structure, most notably deformation twinning. Magnetite grains in samples with shocked quartz show closely spaced sets of straight, lamellar twins in single or multiple orientations (Fig. 2). Twinning is one of the major deformation modes that enable minerals to change shape in response to shock wave passage through geologic materials (e.g., Christian and Mahajan, 1995). Deformation twins have been described in other accessory minerals from shocked rocks including zircon (Erickson et al., 2013), monazite (Erickson et al., 2016), xenotime (Cavosie et al., 2016), and titanite (Timms et al., 2019). Twins described here are consistent with magnetite {111} spinel-law twins, and agree with observations of shock-twinning in spinel when the Hugoniot elastic limit (HEL) is exceeded (Schäfer et al., 1983). Twinning in magnetite was not observed outside the zone of shock metamorphism, thus we conclude the pervasive lamellar twinning is a shock-induced microstructure.

Under experimental shock-conditions, Reznik et al. (2016) reported fracturing/fragmentation, development of microshear bands (5 GPa), mechanical twins (≥10 GPa), kink-bands (30 GPa), as well as transmission electron microscopy-scale amorphization of magnetite. The microstructural observations were associated with decreasing magnetic susceptibility and increasing coercivity of the investigated crystals. Our observations of twinning in magnetite are broadly consistent with that study. In spinel-structured materials, the slip system 1/2 <110>{111} is structurally favored because it comprises the shortest translation vector and the most densely packed lattice plane, and operates both in high-temperature and low strain-rate endogenic processes, and during shock deformation experiments (Schäfer et al., 1983). In experimentally shocked spinel, Schäfer et al. (1983) reported dislocations interpreted as remnants of shock-induced plastic deformation by the slip system 1/2 <110>{111} and {111} mechanical twins. In grains studied here, plastic strain results in systematic misorientation about {111} (Fig. 2f), consistent with 1/2<110>{111} slip in spinel-structured minerals.

Few descriptions of natural shock-induced twins in magnetite have been reported. Cloete et al. (1999) reported <1 μm sized twins in magnetite inclusions in shocked quartz in granitic gneiss from the Vredefort structure (South Africa), and Timms et al. (2019) reported a grain of magnetite with twins in shocked granitoid from the Chicxulub structure (Mexico). Magnetite microstructures formed in shock experiments (Reznik et al., 2016) are on the order of 10s of nanometers, thus much smaller in scale than those reported here. The drastic difference in dimension of twins in our study from the results of Reznik et al. (2016) could result from differences between natural hypervelocity impact events and experimental impact cratering, such as shock pulse duration, geometry of the shock wave, as well as shock impedance, textural features, and pre-shock temperature of target rocks (e.g., Stöffler, 1972; Huffman and Reimold, 1996; Stöffler et al., 2018; Wittman et al., 2021). Increasing grain size is known to result in increased volume fraction of microtwins and microbands in metals and alloys (Murr and Esquivel, 2004). However, given the similarity in size of grains investigated by us and those in Reznik et al. (2016), grain size alone cannot explain observed differences in shock-induced twinning.

Shock impedance has recently been described as the cause of localized pressure amplification for zircon enclosed in less dense minerals (Wittman et al., 2021). We did not observe variations in magnetite twins based on different surrounding phases (typically biotite, plagioclase, hornblende, or titanite), but given the high density of magnetite, local pressure amplifications beyond mean pressure estimates may have occurred.

Chronology of shock features

Twin formation in investigated magnetite grains appears unaffected by non-planar fractures, as we have observed no abrupt terminations of twins at fractures. Instead, twins are in some instances offset by both planar and non-planar fractures, suggesting the fractures post-date twin formation (Fig. 2C, 3; DR Item 6C). Planar fractures may form as twin planes open as tensile cracks during pressure release (e.g., similar to opening of feather features in quartz; Poelchau and Kenkmann, 2011). Plastic strain is constrained to the host crystal between twin sets, and crosscutting twins and lamellae, indicating dislocation slip was active during twinning and after.

Magnetite in sample 69 appear relatively unaffected by alteration, however, grains in samples 21 and 58 are highly altered (alteration was also observed in sample 5; DR item 4, 5). Hematite alteration appears to utilize twin planes and fractures for fluid ingress, as well as crosscutting some twins. Martitization is interpreted to have occurred in hydrothermal systems within the newly formed crater (e.g., Hode et al., 2003). Impact craters on Earth, and other bodies such as Mars, have been subject to hydrothermal alteration (e.g., Osinski et al., 2013). Despite extensive alteration of Siljan magnetite, preserved shock features were identified in all samples from the zone of shock metamorphism, indicating that shocked magnetite can be stable for hundreds of millions of years, even in hydrothermally altered rocks.

Progressive shock metamorphism of magnetite recorded by lamellar twins

The number of twin sets in Siljan magnetite correlates with distance from the crater center, and thus with intensity of shock deformation (Fig. 3). Magnetite grains from sample 69 (15-20 GPa) exhibit up to four sets of twin lamellae, whereas samples subjected to lower shock levels record one to two (rarely three) sets of twin lamellae per grain. Thus, as the magnetite lattice is subjected to higher stress (higher shock pressure), load release happens through twinning in more directions than at lower stress (lower shock pressure). A similar explanation was suggested for increasing number of twins in shocked monazite grains (Erickson et al., 2016), where the number of twins per grain was suggested to be analogous to PDFs in quartz, which exhibit a greater number of PDF orientations at higher shock pressures (e.g., Holm-Alwmark et al., 2018). The largest magnitude of plastic strain (18° of cumulative misorientation) was observed in grains from sample 69, 1.7 km from the crater center.

Significance of shock-induced grain-scale deformation of magnetite

The volume of rock that experiences low pressure (~5-10 GPa) during impact is 2-3 times larger than that which is subject to higher pressures (Poelchau and Kenkman, 2011). Additionally, in eroded or small impact craters, low-pressure deformation may be all that is available for study, especially once ejecta has been removed. There is therefore a need to understand shock effects in the pressure range between quasi-static deformation at the HEL and high shock-pressure indicators (e.g., Poelchau and Kenkmann, 2011). While {111} twins in magnetite are not here considered diagnostic impact features, they can be used to characterize the extent of shock deformation in rocks with a known shock provenance, and thus constrain effects of shock wave propagation and attenuation. Since magnetite occurs in a wide range of rock types, it can also be used as a shock barometer in rocks generally lacking quartz (e.g., limestone, gabbro, and serpentinite).

We have shown that mechanical twins, plasticity, and fracturing are important features of magnetite from target rocks across a relatively wide range of shock pressures, first appearing at low shock pressures (>5 GPa; average 7.2 GPa). Magnetic domain structures in magnetite are sensitive to lattice defects and modifications, caused by plastic deformation (twinning), and other internal stress (e.g., Dunlop and Özdemir, 1997). Twins within experimentally shocked magnetite reported by Reznik et al. (2016) contributed to increasing coercivity in their material. Our results, thus, illuminate processes that can result in impact-modification of magnetic fabrics in crustal rocks on terrestrial planets.

ACKNOWLEDGMENTS

SHA was supported by the Swedish Research Council (grant #2017-06388) and the Royal Physiographical Society in Lund. Thanks to C. Alwmark for help with resolving SEM-related issues. Professional editorial handling by M. Norman, and thorough reviews by A. Wittman and two anonymous reviewers are gratefully acknowledged.

REFERENCES CITED

Barbosa, P. F., and Lagoeiro, L., 2010, Crystallographic texture of the magnetite-hematite transformation: Evidence for topotactic relationships in natural samples from Quadrilátero Ferrífero, Brazil. American Mineralogist, v. 95, p. 118–125, https://doi.org/10.2138/am.2010.3201.

Cavosie, A.J., Montalvo, P.E., Timms, N.E., and Reddy, S.M., 2016, Nanoscale deformation twinning in xenotime, a new shocked mineral, from the Santa Fe impact structure (New Mexico, USA): Geology, v. 44, p.803–806.

Christian, J.W., and Mahajan, S., 1995, Deformation twinning: Progress in Materials Science, v. 39, p. 1–157, https://doi.org/10.1016/0079-6425(94)00007-7.

Cloete, M., Hart, R.J., Schmid, H.K., Drury, M., Demanet, C.M., and Sankar, K.V., 1999, Characterization of magnetite particles in shocked quartz by means electron- and magnetic force microscopy: Vredefort, South Africa. Contributions to Mineralogy and Petrology, v. 137, p. 232–245, https://doi.org/10.1007/s004100050548.

Deer, W.A., Howie, R.A., and Zussman, J., 1992, An introduction to the rock-forming minerals: New York, Wiley, 696 p.

Della Guista, A., Princivalle, F., and Carbonin, S., 1987, Crystal structure and cation distribution in some natural magnetites: Mineralogy and Petrology, v. 37, p. 315–321, https://doi.org/10.1007/BF01161823.

Dunlop, D., and Özdemir, Ö., 1997, Rock Magnetism: Fundamentals and Frontiers: Cambridge, Cambridge University Press, 573 p.

Erickson, T.M., Cavosie, A.J., Moser, D.E., Barker, I.R., and Radovan, H.A., 2013, Correlating planar microstructures in shocked zircon from the Vredefort Dome at multiple scales: Crystallographic modeling, external and internal imaging, and EBSD structural analysis: American Mineralogist, v. 98, p. 53-65, https://doi.org/10.2138/am.2013.4165.

Erickson, T.M., Cavosie, A.J., Pearce, M.A., Timms, N.E., and Reddy, S.M., 2016, Empirical constraints on shock features in monazite using shocked zircon inclusions: Geology, v. 44, p. 635–638, https://doi.org/10.1130/G37979.1.

Estifanos, B., Ståhl, K., Andréasson, P.G., Bylund, G., and Johansson, L., 1997, Norsk Geologisk Tidsskrift, v. 77, p. 119–122.

Ferré, E.C., Zechmeister, M.S., Geissman, J.W., MathanaSekaran, N., and Kocak, K., 2005, The origin of high magnetic remanence in fault pseudotachylites: Theoretical considerations and implication for coseismic electrical currents: Tectonophysics, v. 402, p. 125–139, https://doi.org/10.1016/j.tecto.2005.01.008.

Gattacceca, J., Lamali, A., Rochette, P., Boustie, M., and Berthe, L., 2007, The effects of explosive-driven shocks on the natural remanent magnetization and the magnetic properties of rocks: Physics of the Earth and Planetary Interiors, v. 162, p. 85–98, https://doi.org/10.1016/j.pepi.2007.03.006.

Gilder, S.A., LeGoff, M., Chervin, J.-C., and Peyronneau, J., 2004, Magnetic properties of single and multi-domain magnetite under pressures from 0 to 6 GPa: Geophysical Research Letters, v. 29, p. L10612, https://doi.org/10.1029/2004GL019844.

Hode, T., von Dalwigk, I., and Broman, C., 2003, A hydrothermal system associated with the Siljan impact structure, Sweden—Implications for the search for fossil life on Mars: Astrobiology, v. 3, p. 271–289, https://doi.org/10.1089/153110703769016370.

Holm, S., Alwmark, C., Alvarez, W., and Schmitz, B., 2011, Shock barometry of the Siljan impact structure, Sweden: Meteoritics & Planetary Science, v. 46, p. 1888–1909, https://doi.org/10.1111/j.1945-5100.2011.01303.x.

Holm-Alwmark, S., Rae, A.S.P., Ferrière, L., Alwmark, C., and Collins, G.S., 2017, Combining shock barometry with numerical modeling: Insights into complex crater formation – The example of the Siljan impact structure (Sweden): Meteoritics & Planetary Science, v. 52, p. 2521–2549, https://doi.org/10.1111/maps.12955.

Holm-Alwmark, S., Ferrière, L., Alwmark, C., and Poelchau, M.H., 2018, Estimating average shock pressures recorded by impactite samples based on universal stage investigations of planar deformation features in quartz – Sources of error and recommendations: Meteoritics & Planetary Science, v. 53, p. 110–130, https://doi.org/10.1111/maps.13029.

Holm-Alwmark, S., 2021, Impact cratering record of Sweden—A review, *in* Reimold, W.U., and Koeberl, C., eds., Large Meteorite Impacts and Planetary Evolution VI: Geological Society of America Special Paper 550, p. 1–39, https://doi.org/10.1130/2021.2550(01).

Huffman, A.R., and Reimold, W.U., 1996, Experimental constraints on shock-induced microstructures in naturally deformed silicates: Tectonophysics, v. 256, p. 165–217, https://doi.org/10.1016/0040-1951(95)00162-X.

Jourdan, F., 2012, The $^{40}Ar/^{39}Ar$ dating technique applied to planetary sciences and terrestrial impacts: Australian Journal of Earth Sciences, v. 59, p. 199–224, https://doi.org/10.1080/08120099.2012.644404

Kletetschka, G., Connerney, J.E.P., Ness, N.F., and Acuña, M.H., 2004, Pressure effects on martian crustal magnetization near large impact basins: Meteoritics & Planetary Science, v. 39, p. 1839–1848, https://doi.org/10.1111/j.1945-5100.2004.tb00079.x.

Louzada, K.L., Stewart, S.T., Weiss, B.P., Gattacceca, J., Lillis, R.J., and Halekas, J.S., 2011, Impact demagnetization of the Martian crust: Current knowledge and future directions: Earth and Planetary Science Letters, v. 305, p. 257–269, https://doi.org/10.1016/j.epsl.2011.03.013.

Murr, L.E., and Esquivel, E.V., 2004, Observations of common microstructural issues associated with dynamic deformation phenomena: Twins, microbands, grain size effects, shear bands, and dynamic recrystallization: Journal of Materials Science, v. 39, p. 1153–1168, https://doi.org/10.1023/B:JMSC.0000013870.09241.c0.

Osinski, G.R., Tornabene, L.L., Banerjee, N.R., Cockell, C.S., Flemming, R., Izawa, M.R.M., McCutcheon, J., Parnell, J., Preston, L.J., Pickersgill, A.E., Pontefract, A., Sapers, H.M., and Southam, G., 2013, Impact-generated hydrothermal systems on Earth and Mars: Icarus, v. 224, p. 347–363, https://doi.org/10.1016/j.icarus.2012.08.030.

Pilkington, M., and Grieve, R.A.F., 1992, The geophysical signature of terrestrial impact craters: Reviews of Geophysics, v. 30, p. 161–181, https://doi.org/10.1029/92RG00192.

Poelchau, M.H., and Kenkmann, T., 2011, Feather features: A low-shock-pressure indicator in quartz: Journal of Geophysical Research, v. 116, p. B02201, https://doi.org/10.1029/2010JB007803.

Reimold, W.U., Kelley, S.P., Sherlock, S.C., Henkel, H., and Koeberl, C., 2005, Laser argon dating of melt breccias from the Siljan impact structure, Sweden: Implications for a possible relationship to Late Devonian extinction events: Meteoritics & Planetary Science, v. 40, p. 591–607, https://doi.org/10.1111/j.1945-5100.2005.tb00965.x.

Reznik, B., Kontny, A., Fritz, J., and Gerhards, U., 2016, Shock-induced deformation phenomena in magnetite and their consequences on magnetic properties: Geochemistry, Geophysics, Geosystems, v. 17, p. 2374–2393, https://doi.org/10.1002/2016GC006338.

Schäfer, H., Müller, W.F., and Hornemann, U., 1983, Shock effects in $MgAl_2O_4$-Spinel: Physics and Chemistry of Minerals, v. 9, p. 248–252, https://doi.org/10.1007/BF00309574.

Swedish Geological Survey bedrock map viewer. https://apps.sgu.se/kartvisare/kartvisare-berg-50-250-tusen.html (Accessed 2021-04; In Swedish).

Stephens, M. B., 2020, Introduction to the lithotectonic framework of Sweden and organization of this Memoir, *in* Stephens, M. B., and Bergman Weihed, J., Sweden: Lithotectonic framework, tectonic evolution and mineral resources: Geological Society London, Memoirs, 50, p. 1–18.

Stöffler, D., 1972, Deformation and transformation of rock-forming minerals by natural and experimental shock processes. I. Behavior of minerals under shock compression: Fortschritte der Mineralogie, v. 49, p. 50–113.

Stöffler, D., Hamann, C., and Metzler, K., 2018, Shock metamorphism of planetary silicate rocks and sediments: Proposal for an updated classification system: Meteoritics & Planetary Science, v. 53, p. 5–49, https://doi.org/10.1111/maps.12912.

Timms, N.E., Pearce, M.A., Erickson, T.M., Cavosie, A.J., Rae, A.S.P., Wheeler, J., Wittmann, A., Ferrière, L., Poelchau, M.H., Tomioka, N., Collins, G.S., Gulick, S.P.S., Rasmussen, C., Morgan, J.V., and IODP-ICDP Expedition 364 Scientists, 2019, New shock microstructures, in titanite ($CaTiSiO_5$) from the peak ring of the Chicxulub impact structure, Mexico: Contributions to Mineralogy and Petrology, v. 174, p. 38, https://doi.org/10.1007/s00410-019-1565-7.

Wittman, A., Cavosie, A.J., Timms, N.E., Ferrière, L., Rae, A., Rasmussen, C., Ross, C., Stockli, D., Schmieder, M., Kring, D.A., Zhao, J., Xiao, L., Morgan, J.V., Gulick, S.P.S., and IODP-ICDP Expedition 364 Scientists, 2021, Shock impedance amplified impact deformation of zircon in granitic rocks from the Chicxulub impact crater: Earth and Planetary Science Letters, v. 575, p. 117201, https://doi.org/10.1016/j.epsl.2021.117201.

FIGURE CAPTIONS

Figure 1. Simplified geologic map of the Siljan impact structure (modified after Swedish Geological Survey (SGU) bedrock map viewer (2021); Holm et al., 2011; Holm-Alwmark,

2021). Sample localities are indicated by black dots and corresponding numbers. Ages from SGU bedrock map viewer (2021) and Stephens (2020).

Figure 2. A: BSE image of shocked magnetite aggregate (sample 69, grain #1) intergrown with zircon. B: Cumulative misorientation map showing up to 14° variation across the host and twin boundaries in red. C: Inverse pole figure (IPF) z orientation map. D: High-resolution map of shocked zircon exhibiting one set of shock twin lamellae. Arrows indicate twin orientations in both zircon (zt) and magnetite (t1-3). E: Pole figures plotted as equal area, lower hemisphere projections. F: Crystallographic relationships between twin and host for twins in magnetite and zircon. Pl = plagioclase; Ap = apatite; Afs = alkali feldspar; Mag = magnetite; Bt = biotite; Qz = quartz; Zrn = zircon.

Figure. 3. Progressive shock metamorphism of magnetite with distance from the crater center. Cumulative misorientation maps are shown for representative magnetite in each sample. Special boundaries (yellow) are consistent with topotactic martitization transformation of magnetite to hematite. Twin boundaries in samples 21, 58 and 69 are marked in red. A planar deformation band (PDB) is labeled in sample 58.

[1]GSA Data Repository item 20XXxxx, [EBSD data and additional description of methods], is available online at www.geosociety.org/pubs/ft20XX.htm, or on request from editing@geosociety.org.

Figure 1

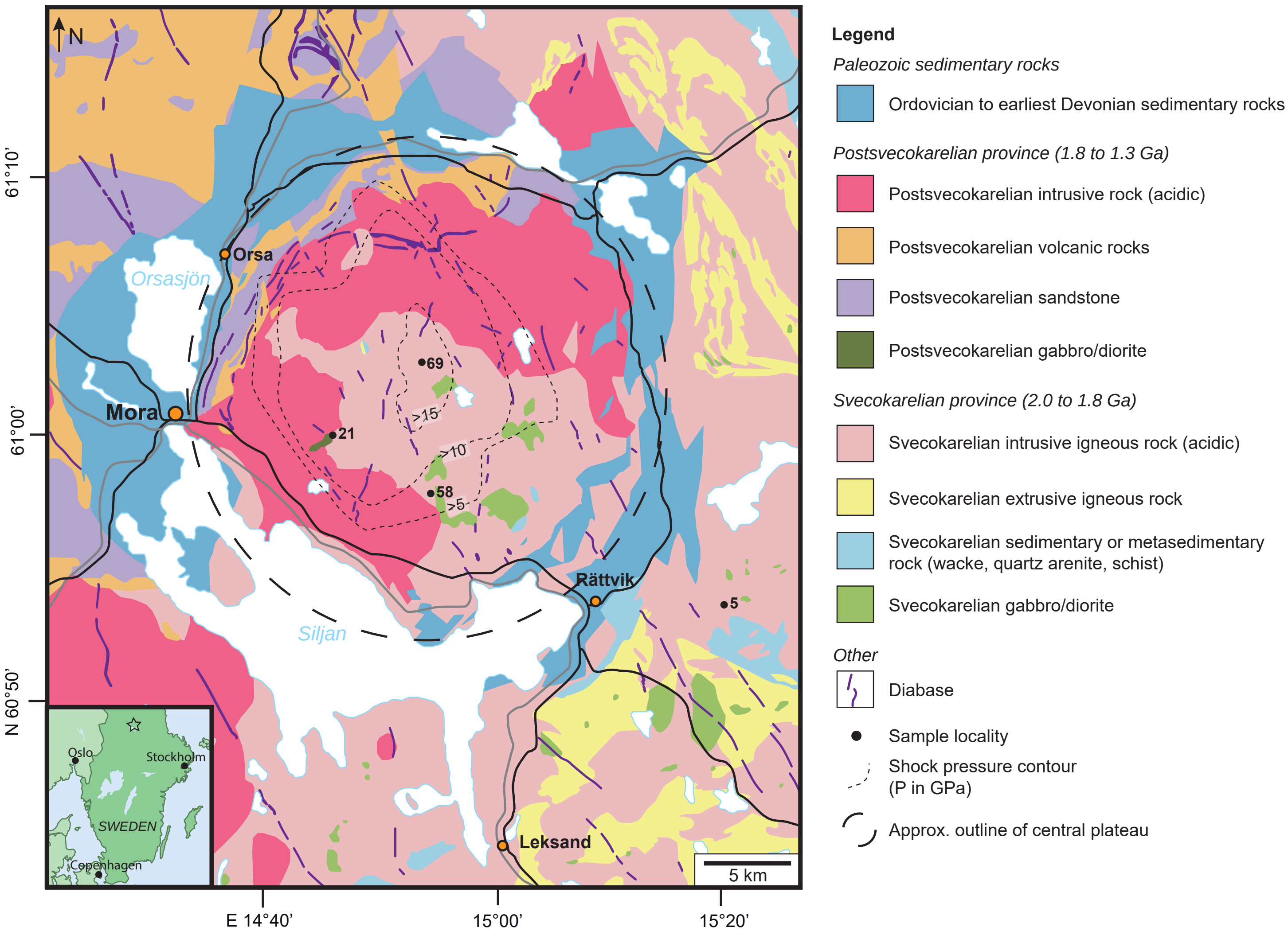

N
Orsa
Orsasjön
Mora
Siljan
Rättvik
Leksand
69
21
58
5
>15
>10
>5
5 km
61°10'
61°00'
N 60°50'
E 14°40'
15°00'
15°20'
Oslo
Stockholm
SWEDEN
Copenhagen
Legend
Paleozoic sedimentary rocks
Ordovician to earliest Devonian sedimentary rocks
Postsvecokarelian province (1.8 to 1.3 Ga)
Postsvecokarelian intrusive rock (acidic)
Postsvecokarelian volcanic rocks
Postsvecokarelian sandstone
Postsvecokarelian gabbro/diorite
Svecokarelian province (2.0 to 1.8 Ga)
Svecokarelian intrusive igneous rock (acidic)
Svecokarelian extrusive igneous rock
Svecokarelian sedimentary or metasedimentary rock (wacke, quartz arenite, schist)
Svecokarelian gabbro/diorite
Other
Diabase
Sample locality
Shock pressure contour (P in GPa)
Approx. outline of central plateau

Figure 2

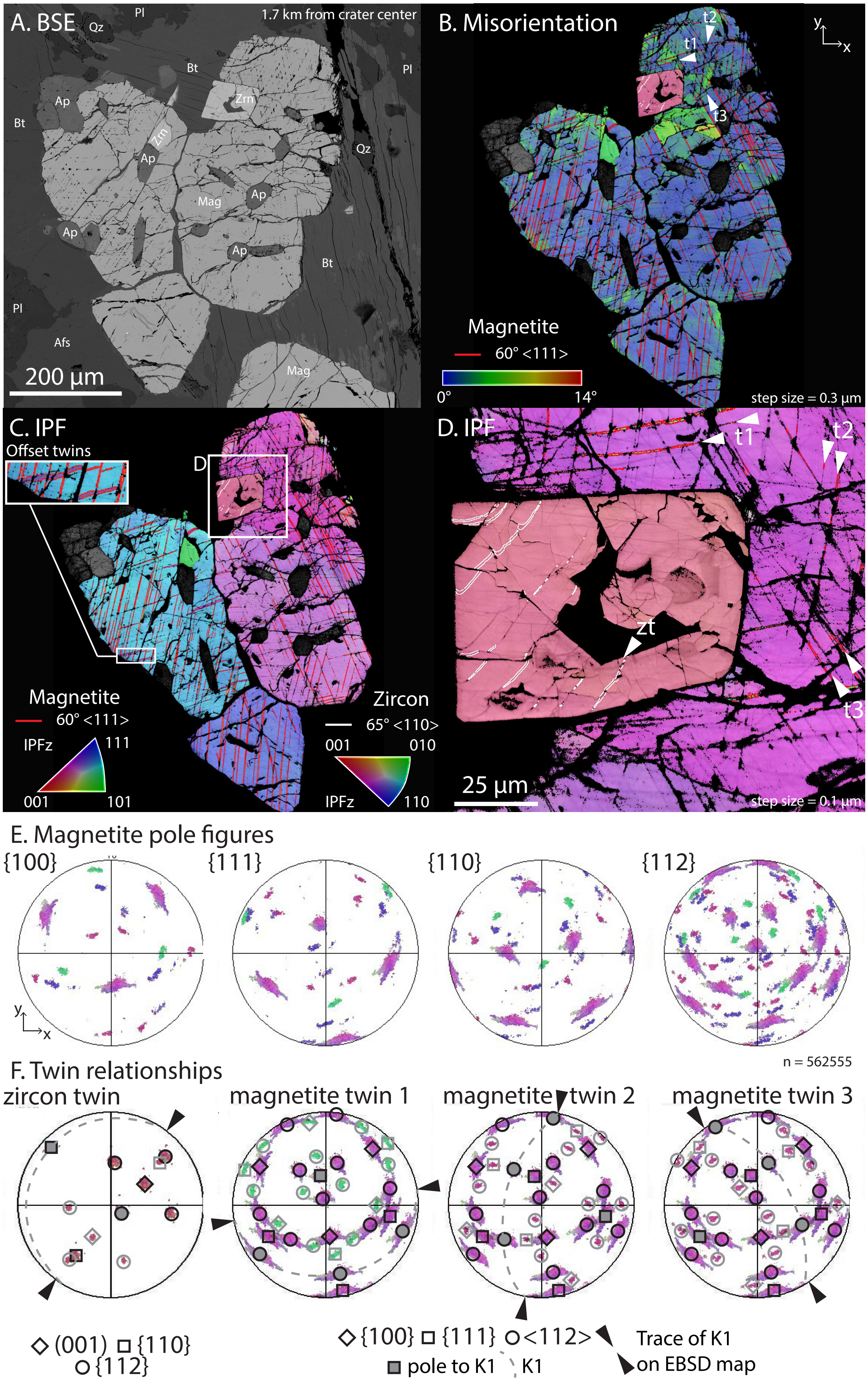
A. BSE
1.7 km from crater center
Qz
Pl
Bt
Ap
Zrn
Mag
Afs
200 µm
B. Misorientation
t1
t2
t3
Magnetite
60° <111>
0°
14°
step size = 0.3 µm
C. IPF
Offset twins
D
Magnetite
60° <111>
IPFz
111
001
101
Zircon
65° <110>
001
010
110
D. IPF
zt
25 µm
step size = 0.1 µm
E. Magnetite pole figures
{100}
{111}
{110}
{112}
n = 562555
F. Twin relationships
zircon twin
magnetite twin 1
magnetite twin 2
magnetite twin 3
(001) {110}
{112}
{100} {111} <112>
pole to K1
K1
Trace of K1
on EBSD map

Figure 3

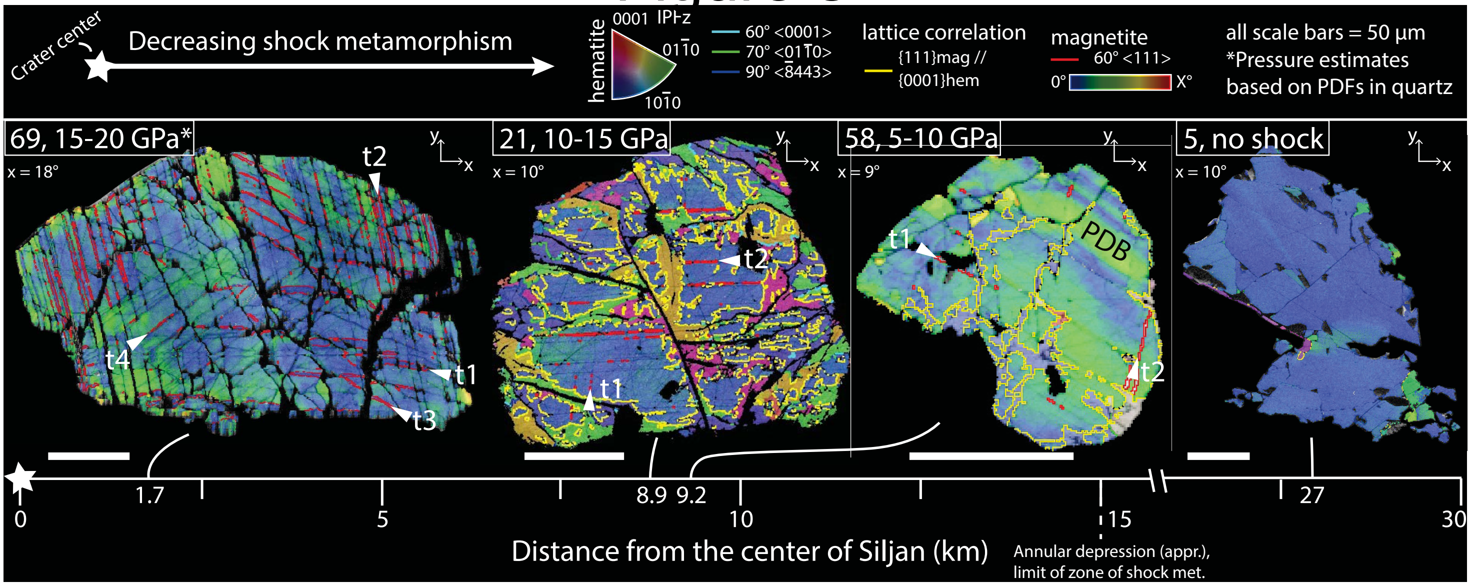

Crater center
Decreasing shock metamorphism
hematite
0001 IPFz
01$\bar{1}$0
10$\bar{1}$0
60° <0001>
70° <01$\bar{1}$0>
90° <$\bar{8}$443>
lattice correlation
{111}mag // {0001}hem
magnetite
60° <111>
0°
X°
all scale bars = 50 µm
*Pressure estimates based on PDFs in quartz
69, 15-20 GPa*
x = 18°
t1
t2
t3
t4
21, 10-15 GPa
x = 10°
t1
t2
58, 5-10 GPa
x = 9°
t1
t2
PDB
5, no shock
x = 10°
y
x
0
1.7
5
8.9
9.2
10
15
27
30
Distance from the center of Siljan (km)
Annular depression (appr.), limit of zone of shock met.

TABLE 1. SAMPLES INVESTIGATED IN THIS STUDY

Sample number	Lithology*	Distance from geographical center (km)	Coordinates[†]	Pressure range (GPa)[§]	Avg. pressure (GPa)[#]	No. of investigated magnetite grains/aggregates in sample	Magnetite observations (Maximum number of sets of twins observed in grains per sample)
69	Hornblende-biotite granite	1.7	N61°03.051'; E014°53.612'	15-20	16	6	Twins (4)
21	Hornblende-biotite granite	8.9	N60°59.569'; E014°46.760'	10-15	10.6	3	Twins (3)
58	Hornblende-biotite granite	9.2	N60°57.409'; E014°54.355'	5-10	7.2	2	Twins (2)
5	Hornblende-biotite granite	27.4	N60°53.270'; E015°18.863'	No shock**	No shock**	3	No twins

*All samples are coarse-grained, porphyric granitoids that contain alkali feldspar, quartz, plagioclase, hornblende, and biotite with minor magnetite, titanite, zircon, and apatite.

[†]Coordinates are in SWEREF 99 (WGS 84).

[§]Pressure range estimate, see Holm et al. (2011).

[#]Pressure estimate as an average calculated from pressure values of each individual quartz grain in the sample, based on the PDF population in each grain, see Holm-Alwmark et al. (2018).

**Sample is from outside of zone of PDF occurrences in quartz and shatter cone observations.